Adsorption of Semiflexible Polymers on Flat, Homogeneous Surfaces

T. Sintes*

Instituto Mediterráneo de Estudios Avanzados, IMEDEA (CSIC−UIB), E-07071 Palma de Mallorca, Spain

K. Sumithra and E. Straube

FG Theoretische Physik, FB Physik, Martin Luther Universitaet, D-06099 Halle-Wittenberg, Germany

Received March 21, 2000

ABSTRACT: We investigated the problem of adsorption of a single semiflexible polymer chain on to a planar, homogeneous surface using off-lattice Monte Carlo simulations. Adsorption characteristics were studied at different temperatures for chains of various stiffnesses. We have found that the stiffer chains adsorb more onto the surface and the adsorption transition takes place at a higher temperature when compared to that of the flexible chains. As stiffness increases, the adsorption transition is found to be sharper. The computed persistence length is found to grow linearly for small values of the bending energy, while for higher values, it shows a square root dependence. In the ground state, the parallel size of the stiffer chain is found to be much larger than that of the corresponding flexible polymer chain. The classical scaling laws for the flexible chains were tested for the stiffer chains and found that they are well obeyed, indicating that the universal properties of the chain measured over its whole dimension are unaffected by the local stiffness of the chain.

I. Introduction

Polymer chain adsorption at surfaces, both homogeneous[1] and heterogeneous,[2,3] has been a topic of great experimental and theoretical interest, owing to its tremendous applications in science and technology. These applications include adhesion, gel permeation chromatography, etc. A vast majority of the theoretical investigation has been concentrated on the adsorption of ideal flexible polymer chains, where free rotation about the backbone is possible. Adsorption characteristics as well as the universal properties of such chains on planar, on homogeneous,[4] and on chemically heterogeneous surfaces are now well-known.[5] In reality, many polymers are rigid to certain extent due to reasons such as electronic delocalization and steric effects. A few important examples of such stiff chains, from biology, are actin filaments, microtubules, DNA, and collagen. On a local length scale, the stiffness is very prominent and is expected to cause significant changes in the macromolecular properties. Since the free rotations about the chain backbone are restricted, the chain statistics cannot be described accurately by the conventional models for describing flexible chains.

The stiffness of a semiflexible polymer chain is intermediate between that of random coils and rigid rods. The statistical mechanics of such chains were first formulated, about 50 years ago, by Kratky and Porod[6] and are still considered as a nontrivial problem. There have been some recent developments in the area of semiflexible chains at interfaces[7] and a very few at surfaces.[8−10] Kramarenko et al., while discussing adsorption of flexible polymer chains on flat surfaces, have briefly visited through stiffer chains, using molecular dynamics simulations. But how the adsorption characteristics are changed with varying degrees of stiffness or how the universal properties are valid are still unclear. Therefore, a proper understanding requires a more detailed study.

The purpose of the current investigation is to shed light on the adsorption characteristics of a semiflexible polymer chain on a flat homogeneous, attracting surface. We present here how the adsorption characteristics are changed by increasing stiffness of the chain and how the universal scaling laws apply here. We measure adsorption energy as well as persistence length radius of gyration and its components at various temperatures, for chains of various degrees of stiffnesses.

II. Model and Simulation Technique

We have simulated the adsorption of a semiflexible polymer chain on an homogeneous surface using off-lattice Monte Carlo methods. We have considered a polymer chain confined in a unit box with periodic boundary conditions in the $x-y$ domain. The length of the cell is chosen to be at least twice the chain length, N, and an impenetrable planar surface is set at the $z = 0$ plane. The polymer chain is represented by a *pearl-necklace model*[11] containing N beads of diameter σ.

The stiffness of the polymer chain is usually characterized by the arc length over which the tangential correlations of the contour decay to $1/e$ and is commonly referred to as the persistence length l_p. Or, in other words, it can be considered as the distance over which the polymer chain is stiff. We introduce the stiffness through the bending potential U_B given by[12]

$$U_B = \sum_{\theta} \kappa(1 + \cos\theta)^2 \qquad (1)$$

where θ is the bond angle between any three consecutive sites and κ is the bending constant.

Monomers that are two or more beads apart interact through a steric hard-core potential of the form

$$U_{\text{steric}} = \sum_{i,j=1}^{N} V(r_{ij}) \qquad (2)$$

* To whom correspondence should be addressed.

10.1021/ma000493s CCC: $20.00
Published on Web 01/26/2001

where V is given by

$$V(r_{ij}) = \begin{cases} 0, & \text{for } |\mathbf{r}_i - \mathbf{r}_j| > \sigma \\ \infty, & \text{for } |\mathbf{r}_i - \mathbf{r}_j| < \sigma \end{cases} \quad (3)$$

Monomer units have an attractive interaction with the impenetrable surface at $z = 0$ with adsorption energy $\epsilon < 0$. Thus, we define an adsorption potential U_A as

$$U_A = n_c\epsilon \quad (4)$$

with n_c being the number of i-monomers such that their z-coordinate verifies $0 < z_i < \sigma$. The total energy of the system will contain the above contributions and is written as

$$U = U_A + U_B + U_{steric} \quad (5)$$

The initial configuration of the self-avoiding polymer is randomly generated with one monomer attached to the surface $z = 0$. Next, the polymer is tried to move by randomly executing a reptating type motion in a forward or reverse direction, or by selecting an individual monomer which position can be rotated, around the axis connecting the previous and following monomer in the chain, an arbitrary angle between 0 and 2π. Chain ends just perform random wiggling motions. Each move is accepted according to the standard Metropolis Monte Carlo algorithm, $\exp(-\Delta U/k_BT) > \eta$, where $0 < \eta < 1$ is a random number. A link-cell method[13] has been implemented in the algorithm to efficiently check ΔU. For the rest of the paper we will measure the temperature T in units of ϵ/k_B and hence $T \equiv k_BT/|\epsilon|$.

At very high temperatures or equivalently at low adsorption energies, the chain has a tendency to diffuse into the bulk. We prevent this by forcing the polymer to have at least one monomer attached to the surface. However, one does not expect any significant change in the statistical properties of the adsorbed chain at low temperatures. We define one Monte Carlo step (MCS) as N trials to move the chain. The system has been equilibrated for 5×10^5 MCS. Subsequently, the number of monomers in contact with the surface, E, is evaluated every 10 MCS. The results have been finally averaged over 10^6 measures.

III. Results and Discussions

We have estimated the average adsorption energy per monomer E/N as a function of temperature T for various chain lengths N and for various degrees of the stiffness parameter κ. The flexible chain limit corresponds to the value of $\kappa = 0$.[15] We have investigated different chain lengths, $N = 25$, 50, 75, 100, 150, 200, 250, and 500 for different rigidities, $\kappa = 1$, 5, 10, and 30.

The variation of adsorption energy as a function of temperature for $N = 100$ and for different stiffnesses are given in Figure 1. The adsorption energy per monomer E/N shows a monotonic increase with a decrease in temperature for all the cases. It is clear that the energy undergoes significant changes near the critical adsorption temperature $T_c(N)$. At very low temperatures, E/N approaches unity as is expected. Similar qualitative behavior is exhibited by all other values of N.

We have found that the adsorption transition takes place at a higher temperature as the rigidity of the chain increases. This is not surprising since stiffer chains, because of restricted rotations, lose less entropy compared to the flexible chains while adsorbing on to the surface. Since $T_c(N)$ depends on the stiffness, we denote it by the notation $T_c(N,\kappa)$. For all chain lengths, the stiffness dependence is obvious at temperatures below the transition temperatures. The stiffness dependence of adsorption energy is clear from Figure 2, where we plot E/N as a function of κ for few temperatures for $N = 100$. The adsorption energy increases with κ as expected.

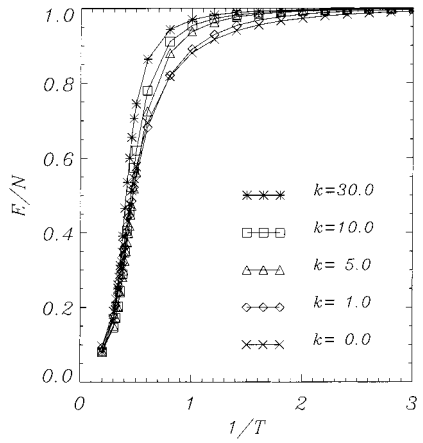

Figure 1. Average energy of adsorption of the polymer chain E/N vs $1/T$ for $N = 100$ and different stiffness parameter κ.

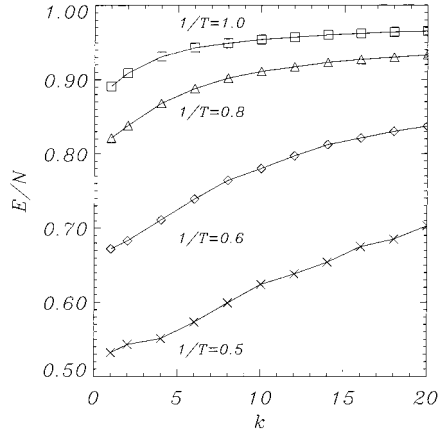

Figure 2. E/N vs κ for few temperatures for $N = 100$.

The transition temperatures, $T_c(N,\kappa)$ for each N and κ are determined from the temperature corresponding to the maximum of the specific heat data. An example plot of the specific heat as a function of temperature for $N = 100$ for different κ is shown in Figure 3. As κ increases, it is obvious that the maximum of the curves shift to higher temperatures, indicating higher transition temperatures. It is also clear that the adsorption transition becomes more sharper as stiffness is increased. To make clear the stiffness dependence of the transition temperature, we plot $T_c(N,\kappa)$ as a function for N for various stiffnesses κ in Figure 4. It is obvious that for each N, the transition temperature is increased with an increase in the rigidity.

To obtain the $T_c(\infty,\kappa)$, the transition temperature for the infinite chain length, the $T_c(N,\kappa)$ values are plotted as a function of $N^{-\phi}$ in Figure 5, where ϕ is the critical crossover exponent. The value of ϕ is taken as 0.59, the classical one for the adsorption of homopolymers on a flat surface.[4] We obtained the values of $T_c(\infty,\kappa)$ by the extrapolation of the curves by least-squares fitting of

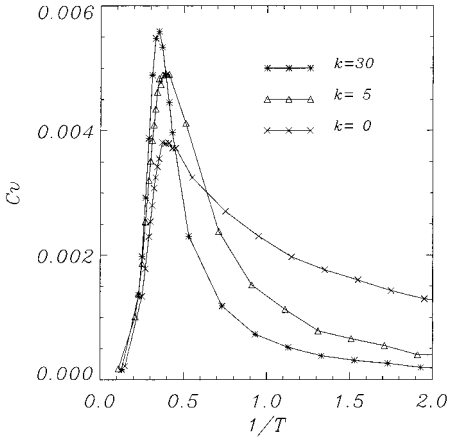

Figure 3. Specific heat of the chain as a function of $1/T$ for $N = 100$ and for different stiffnesses κ.

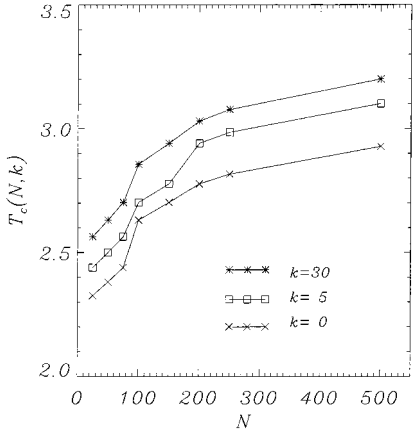

Figure 4. Transition temperatures $T_c(N,\kappa)$ as a function for N for various stiffnesses κ.

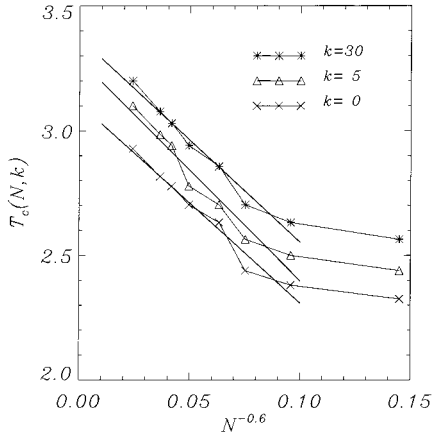

Figure 5. Transition temperatures $T_c(N,\kappa)$ for different N as a function of $N^{-\phi}$.

the data to very large N, denoted by the solid line in Figure 5. The flexible chain adsorption corresponds to the lowermost curve in the figure and the upper lines are for chains with different rigidities.

An important measure of the chain stiffness is given by the persistence length l_p. It can be obtained from the evaluation of the oriental correlation function

$$\langle \mathbf{u}(r)\cdot\mathbf{u}(0)\rangle = \exp(-r/l_p) \tag{6}$$

where $\mathbf{u}(r)$ is the unit vector tangent to the chain at position r. In Figure 6we represent l_p vs $1/T$ for different

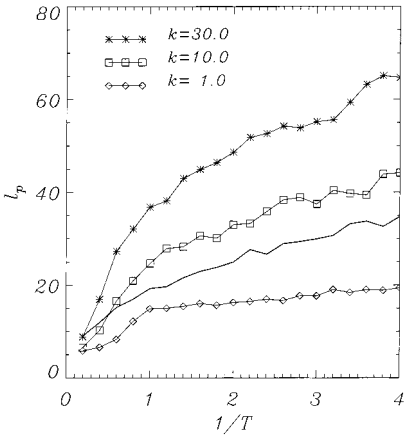

Figure 6. Persistence length as a function of $1/T$ for $N = 100$ and different stiffness parameters κ. Solid line: nonadsorbed 3-d polymer chain for $\kappa = 30$.

values of the stiffness parameter and for a chain length $N = 100$. We note how l_p increases with κ and $1/T$. To find the persistence length we define γ to be the valence angle between two neighboring segments that are separated by the bond length b, therefore

$$\langle \mathbf{u}(r_{i+1})\cdot\mathbf{u}(r_i)\rangle = \langle \cos\gamma\rangle$$

and $\gamma = \pi - \theta$. Since $b \ll l_p$, we can write

$$\langle \cos\gamma\rangle \cong 1 - b/l_p,$$

and

$$\langle \cos\gamma\rangle = \frac{\int_{-1}^{1} \mathrm{d}(\cos\gamma)\cos\gamma \mathrm{e}^{-U_B/T}}{\int_{1}^{1} \mathrm{d}(\cos\gamma)\mathrm{e}^{-U_B/T}}$$

with U_B being the bending potential (eq 1). The solution for l_p has the limiting cases

$$l_p \sim \kappa/T, \text{ for } \kappa/T \to 0$$

and

$$l_p \sim \sqrt{\kappa/T}, \text{ for } \kappa/T \to \infty$$

In Figure 7 we present a log−log plot of l_p as a function of κ/T. We can observe the two regimes described above. For high temperatures, l_p grows linearly with κ/T reproducing the results of the Kratky−Porod model.[14] At smaller temperatures we observe a power-law dependence with κ/T, $l_p \sim (\kappa/T)^{\alpha}$. The best fit to our data gives $\alpha = 0.45 \pm 0.05$, which is in agreement with the expected theoretical behavior. It is remarkable to note that the transition between the two regimes takes place at $T \approx T_c(\kappa)$. For the sake of comparison, we have also studied the case of a free (nonadsorbed) 3-dimensional polymer chain with $\kappa = 30$ and $N = 100$. The result corresponds to the solid line plotted in Figure 6. The persistence length is found to be larger in the adsorbed state. This result is expected due to the more restricted available configurations for the semiflexible chain while adsorbing on to the surface. However, qualitatively, the square root dependence with κ is still maintained as it is shown in Figure 7 (dashed line).

A. The Scaling Analysis. To examine the critical adsorption properties of the semiflexible chain, we

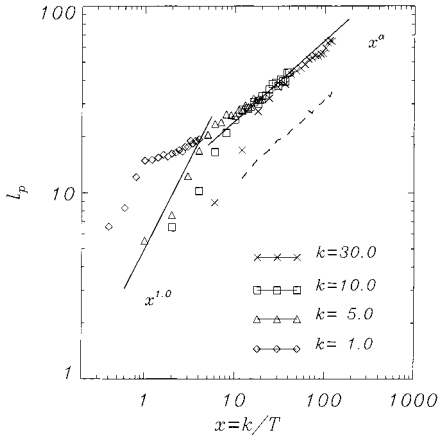

Figure 7. Persistence length as a function of κ/T for $N = 100$. The solid lines indicate the two observed regimes. The dashed line corresponds to the nonadsorbed 3-d polymer chain for $\kappa = 30$.

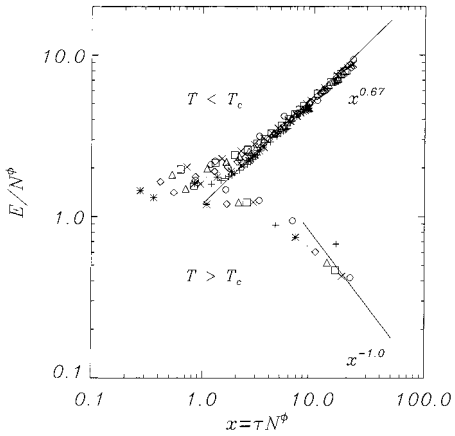

Figure 8. The log−log plot of the scaling function E_N/N^{ϕ} vs the scaling argument τN^{ϕ} for $T < T_c(\infty,\kappa)$, for $\kappa = 0$. The lower part is for $T > T_c(\infty,\kappa)$ for $\kappa = 0$. The symbols refer to the chain length: $N = 25$ (+); $N = 50$ (*); $N = 75$ (●); $N = 100$ (◇); $N = 150$ (△); $N = 200$ (□); $N = 250$ (×); $N = 500$ (○). Straight lines indicate the asymptotic limit.

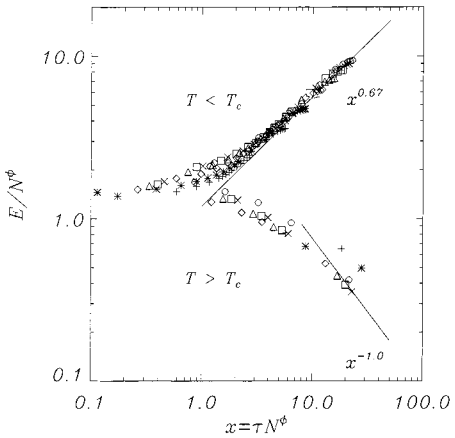

Figure 9. Same as Figure 8 for $\kappa = 5$.

assumed initially the scaling *ansatz* for the flexible homopolymers. It is reasonable to expect that at large length scales, a semiflexible polymer chain in a good solvent behaves like a flexible chain with excluded volume statistics. Only, in the case where the persistence length is comparable to the chain length, we expect the statistics to differ from that of flexible chains. Using the values of $T_c(\infty,\kappa)$, we did a scaling analysis of the data for the energy that depends on the well-known exponent $\nu = 0.59$ and the scaling variable $= \tau N^{\phi}$. For a given value of the stiffness, the cross over scaling for the energy is given by

$$E/N^{\phi} = h(\tau N^{\phi}) \tag{7}$$

where $\tau = (T - T_c(\infty,\kappa))/T_c(\infty,\kappa)$ is the temperature distance to the critical temperature $T_c(\infty,\kappa)$, below which a finite fraction of monomers is on the surface. In eq 7, the scaling function obeys the critical properties

$$h(x) \propto \begin{cases} x^{-1}, & x \to \infty \\ \text{const}, & x \to 0 \\ |x|^{(1-\phi)/\phi}, & x \to -\infty \end{cases} \tag{8}$$

and the corresponding asymptotic behavior ($N \to \infty$) is given by

$$E/N \propto \begin{cases} 0, & T \geq T_c(\infty) \\ |\tau|^{(1-\phi)/\phi}, & T < T_c(\infty) \end{cases} \tag{9}$$

The log−log plot, which gives the scaling analysis of the energy is given in Figure 8 for the flexible polymer chain. This was done to check the validity of our program in reproducing the classical scaling relationships. It is clear from the plot that the conventional scaling law is well obeyed by our Monte Carlo data. We obtained a slope of 0.67 ± 0.02 for $T < T_c(\infty)$ and -0.96 ± 0.02 for $T > T_c(\infty)$ in good agreement with the prediction of eq 8. This confirms, as in the previous studies,[15] the value of 0.59 for the crossover exponent ϕ. A similar analysis is done for the energy data of the semiflexible chains. As the plots for the flexible and semiflexible data lay in a parallel manner very close to each other in the scaling plot, we give a separate plot for the semiflexible case in Figure 9. We get collapsed set of data for all N and straight lines are drawn to indicate the asymptotic limit. The straight lines in the plots give the same asymptotic slopes given by the scaling laws in eq 8, both for low- and high-temperature regimes.

It is interesting to note that the universal scaling laws are unaffected by the stiffness of the semiflexible chain. This is quite reasonable as the stiffness of the chain is a local property and does not affect the universal properties of the chain. The universal asymptotic laws are derived on length scales corresponding to the whole macromolecular dimension where the stiffness, which is a local property, does not play a significant role for $l_p \ll N$.

We have carried out a similar scaling analysis for the parallel $\langle R_{||}^2 \rangle$ and perpendicular $\langle R_{\perp}^2 \rangle$ components of the mean squared radius of gyration. The scaling behavior for these components are given by

$$\langle R^2 \rangle = N^{2\nu} f^2(\tau N^{\phi}) \tag{10}$$

$$\langle R_{\perp}^2 \rangle = N^{2\nu} f_{\perp}^2(\tau N^{\phi}) \tag{11}$$

and

$$\langle R_{||}^2 \rangle = N^{2\nu} f_{||}^2(\tau N^{\phi}) \tag{12}$$

The scaling functions $f_{\perp}(x)$ and $f_{||}(x)$ have the following asymptotic behavior[4]

$$f_{\perp}(x) \propto \begin{cases} \text{const}, & x \to \infty \\ \text{const}, & x \to 0 \\ |x|^{-\nu/\phi}, & x \to -\infty \end{cases} \tag{13}$$

and

$$f_{\parallel}(x) \propto \begin{cases} \text{const}, & x \to \infty \\ \text{const}, & x \to 0 \\ |x|^{(\nu_{d=2}-\nu)/\phi}, & x \to -\infty \end{cases} \tag{14}$$

where $\nu_{d=2} = {}^3/_4$ and $\nu \approx 0.59$ are the correlation length exponents for two and three dimensions, respectively. In Figure 10 we give the a double log plot of $\langle R_{\parallel}^2\rangle/N^{2\nu}$ and $\langle R_{\perp}^2\rangle/N^{2\nu}$ as a function of τN^{ϕ} for both the flexible and the semiflexible chains together. It is interesting to note that the scaled data are laying parallel to each other, indicating that the we have the same value of the slope for the collapsed data for both the components of radius of gyration as in the flexible case. The slope gives the values 0.5 ± 0.02 and -2 ± 0.02 for the parallel and for the perpendicular components.

It is not difficult to understand why semiflexible chains exhibit the same scaling law as that of flexible polymer chains. The persistence length of a long semiflexible chain is much smaller compared to the total contour length of the chain. Therefore, it is reasonable to treat it as a flexible chain in the asymptotic limit. On the other hand, on length scales smaller than the persistence length, the semiflexible chain can be treated as an array of rods, and on these local scales, they exhibit different properties. For example, the chain adsorption is more favored by the stiffer chains when compared to that of flexible chains.

B. The Size of the Adsorbed Chain. The size of the adsorbed chain shows interesting effects as a result of the stiffness. In Figure 11, we plot the temperature dependence of the parallel and perpendicular sizes for flexible as well as for semiflexible chains with various rigidities and for $N = 100$. The perpendicular component of the radius of gyration shows a smooth transition to the completely adsorbed state as the temperature is decreased, and it is clear from the scaling plot in Figure 10. The parallel size of the polymer shows a smooth increase in size as temperature is decreased. The expected increase in the case of adsorbed flexible chain is obviously due to the strong excluded volume interactions. It is clear from Figure 11 that the lateral size of the polymer shows tremendous increase as a result of the stiffness. In this case, local stiffness also contributes to the increase. This happens because only certain types of realizations are possible for the semiflexible chain where the chain is more extended than in flexible case, due to the backbone stiffness, when it is completely adsorbed.

This can also be understood in terms of the persistence length l_p, which is a measure of the stiffness of the chain. When the stiffness is appreciable, l_p, the distance over which the chain is stiff, will also be sufficiently large, which will not allow compact conformations for the stiffer chain which a flexible chain can achieve easily because of its flexibility. To illustrate this point, we show two dimensional snapshots of the adsorbed configuration of the flexible and a stiffer chain with the stiffness parameter $\kappa = 10$, for $N = 100$ in Figures 12 and 13, respectively. It is clear that the chain is in a more extended configuration in the semiflexible case, while it is more compact in the flexible chain where rotations are free.

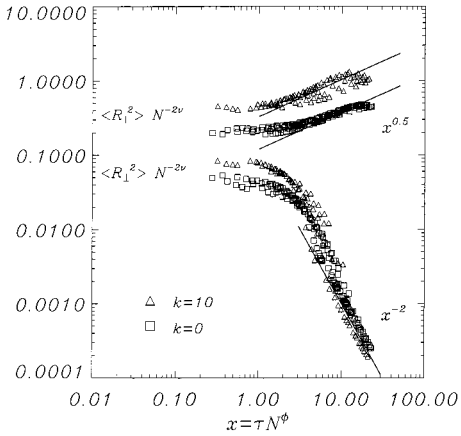

Figure 10. The log−log plot of the scaling function $\langle R_{\parallel}^2\rangle/N^{2\nu}$ and $\langle R_{\perp}^2\rangle/N^{2\nu}$ as a function of the scaling argument τN^{ϕ} for $\kappa = 0$ and $\kappa = 10$. In both cases the value of the chain length ranges from $N = 25$ to $N = 500$.

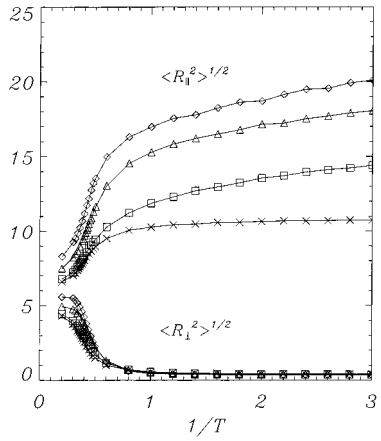

Figure 11. Parallel and perpendicular components of the radius of gyration as a function of temperature $1/T$ for $N = 100$. The symbols refer to the chain stiffness: $\kappa = 0$ (×); $\kappa = 1$ (□); $\kappa = 5$ (△); $\kappa = 10$ (◇).

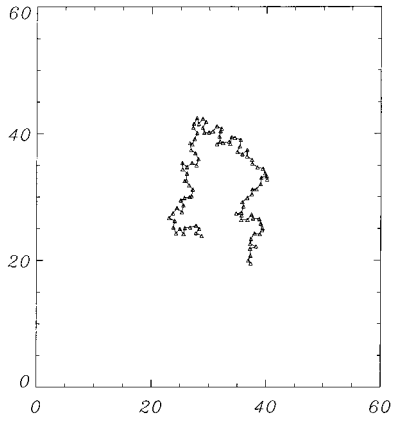

Figure 12. Two-dimensional snapshot of the flexible chain on the surface for $N = 100$ and $1/T = 4.0$.

IV. Summary and Conclusions

In our analysis, we have found that the stiffer polymer chains adsorb more to the surface when compared to the flexible chains. This finding was also reported by Kramenko et al.[9] who modeled stiffness as change in the Kuhn length l of the chain. As a result of the restricted rotation about the single bonds connecting the monomers, they lose much less entropy compared to the flexible chains while adsorbing to the surface. The

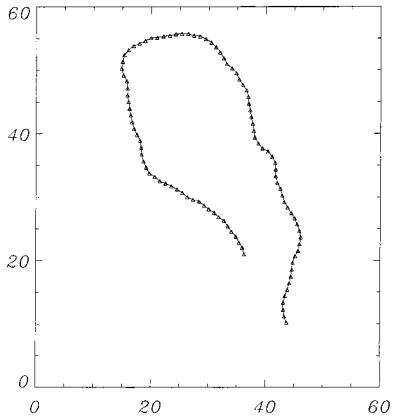

Figure 13. Two dimensional snapshot of a stiffer chain ($\kappa = 10$) on the surface for $N = 100$ at $1/T = 4.0$.

adsorption transition for the stiffer chains are found to occur at higher temperatures as a consequence. We have computed the persistence length as a function of κ and T finding two asymptotic regimes. At high temperatures, l_p grows linearly with κ/k_BT, reproducing the results of the Kratky−Porod model. At smaller temperatures, however, the persistence length follows a square root dependence. It is remarkable to note that the transition between the two regimes takes place at $T \approx T_c(\kappa)$. The same qualitative behavior is observed for a free (nonadsorbed) 3-dimensional polymer chain; however, the magnitude of the persistence length is smaller when compared to the corresponding adsorbed one.

We have checked the validity of the classical scaling laws for the flexible chain adsorption for the semiflexible chain problem. We found that they are well obeyed, proving the crossover exponent of $\phi = 0.59$. The stiffness of a semiflexible chain is more a local property, and for chains whose length is much larger than the persistence length l_p, the properties measured over the entire dimension of the polymer chain, such as the universal scaling laws, remain unaffected. It might be possible to introduce the stiffness, through the change in the persistence length, in the scaling relations, so that one could write universal scaling laws for stiff chains. This last point, however, has been left for future studies.

The local stiffness of the polymer chain is expected to change polymer properties on length scales corresponding to the persistence length of the polymer chain. For example, the lateral size of the polymer shows appreciable increase when compared to that of the flexible chains. This can be attributed to the chain stiffness, because of which the chain is unable to attain compact configurations like in the flexible case and remain more extended.

Acknowledgment. We are grateful to S. Stepanow and K. L. Sebastian for enthusiastic discussions. Financial support to T.S. from DGES (Spain) Project No. PB97-0141-C02-01 is gratefully acknowledged. K.S. is grateful to the Graduiertenkollegs "Polymerwissenschaften" (supported by DFG) for financial support in the form of a postdoctoral fellowship.

References and Notes

(1) de Gennes, P.-G. *Rep. Prog. Phys.* **1969**, *32*, 187.
(2) Sebastian, K.-L.; Sumithra, K. *Phys. Rev. E* **1993**, *47*, R32; *J. Phys. Chem.* **1994**, *98*, 9317.
(3) Baumgaertner, A.; Muthukumar, M. *J. Chem. Phys.* **1991**, *94*, 4062.
(4) Eisenriegler, E. *Polymers near Surfaces*; World Scientific: Singapore, 1993.
(5) Sumithra, K.; Baumgaertner, A. *J. Chem. Phys.* **1998**, *109*, 1540.
(6) Kratky, O.; Porod, G. *Recl. Trav. Chim. Pays-Bas* **1949**, *68*, 1106.
(7) Morse, D.-C.; Fredrickson, G.-H. *Phys. Rev. Lett.* **1994**, *73*, 3235.
(8) van der Linden, C.-C.; Leermakers, F.-A.; Fleer, G.-J. *Macromolecules* **1996**, *29*, 1172.
(9) Kramarenko, E.-Yu; Winkler, R.-G.; Khalatur, P.-G.; Khokhlov, A.-R.; Reineker, P. *J. Chem. Phys.* **1996**, *104*, 4806.
(10) Kuznetsov, D.-V.; Sung, W. *Macromolecules* **1998**, *31*, 2679.
(11) Baumgaertner, A. In *Applications of the Monte Carlo Method in Statistical Physics*, 2nd. ed.; Binder, K., Ed.; Topics in Current Physics 36; Springer-Verlag: Berlin, 1987.
(12) Xiang, T. *Biophys. J.* **1993**, *65*, 1108.
(13) Allen, M.; Tildesley, D. *Computer Simulation of Liquids*; Clarendon: Oxford, England, 1987.
(14) Grosberg, A.-Yu; Khokhlov, A.-R. *Statistical Physics of Macromolecules*; AIP Series in Polymers and Complex Materials; AIP: New York, 1994.
(15) Eisenriegler, E.; Kremer, K.; Binder, K. *J. Chem. Phys.* **1982**, *77*, 6296.

MA000493S